The Tracking and Prediction of High Intensity Rainstorms

RAFFAELE BOLLA[a], GIORGIO BONI[b], PAOLO LA BARBERA[b], LUCA LANZA[b], MARIO MARCHESE[a] and SANDRO ZAPPATORE[a]

[a]Dept. of Communications, Computer and System Science, University of Genova, Opera Pia 13, 16145 Genova, Italy; [b]Institute of Hydraulics, University of Genova, Montallegro 1, 16145 Genova, Italy

The paper addresses some concepts and issues relevant to the use of satellite imagery, as provided by the infrared radiometers flying on board geostationary orbiting platforms, in the tracking and prediction of typical mid-latitude Mesoscale Convective Complexes (MCCs) associated with high intensity rainstorms over the Mediterranean area. The predictive content of sequences of Meteosat half-hourly images is exploited in this work, aiming at the development of storm identification and cloud tracking procedures suitable for operational use in flash flood forecasting applications. Though relying essentially on image processing techniques, the cloud tracking approach seems quite useful in the short term prediction of the dynamics of MCCs as the resolution scale of the temporal sampling provided by the satellite sensor is short enough to ensure that abrupt changes in the cloud characteristics are not likely to occur between two subsequent images. Some studies are presented to show the potential of the procedure and the evidence of strong interactions between the synoptic atmospheric dynamics and local enhancing factors (e.g. thermal effects and orography) in triggering convection.

It is concluded that, in the case of small size catchment hydrology, cloud tracking techniques play a role in supporting the assessment of the risk of flooding, provided that no quantitative rainfall estimates are addressed, but cloud cover and cloud dynamics parameters are used within a probabilistic approach to flood hazard assessment at the regional scale.

I. INTRODUCTION

The potential information content of satellite imagery as obtained from radiometers borne on geostationary orbiting platforms has drawn the attention of the scientific community since the late 1960s, when the first experimental satellites (i.e. the Applications Technology Satellites ATS-I and ATS-III) started providing sequences of images of the Earth and its atmosphere from space. This allowed

meteorologists to observe the dynamics of cloud systems and cloud texture from a revolutionary new perspective. The European scientific community has been widely involved in the exploitation of remotely sensed data since the mid-1970s: the European Space Agency (ESA) Meteosat Programme was initiated operationally in 1977 (Mason, 1981).

The information on the reflected radiances and the radiance temperatures of the top of the clouds, as provided by radiometers operating in the visible (VIS) and thermal infrared (IR) bands on board geostationary orbiting satellites, has been used for many different applications including meteorological studies and flash flood forecasting procedures. Algorithms have been developed in order to provide empirical estimates of the average rainfall intensities over wide areas (see D'Souza *et al.*, 1990 for a review of such methods) as well as to identify and track potentially hazardous cloud systems during their evolution at the synoptic scale (Lanza and Conti, 1995). Several methods have been developed to derive the dynamical parameters related to cloud aggregates with different storm characteristics (convective storms, tornadoes, etc.).

The use of satellite rainfall estimation algorithms is not often expected to provide any significant improvement in flood forecasting when the hydrology of large size catchments and smooth geomorphologic landscapes is operationally concerned. In this case, indeed, traditional rainfall estimation techniques and hydrometric warnings should provide the desired accuracy and be quite acceptable lead times. However, the typical land forms of coastal Mediterranean areas, characterized by steep slopes and small to medium size catchments (10–100 km^2 with a few cases in the 1000 km^2 class), make traditional flood forecasting procedures useless in such regions.

The temporal scale of the hydrological response to high intensity rainfall in the catchments of interest is of the same order of magnitude as the response time requested by the social environment in order to put in action precautionary measures in densely urbanized areas (Siccardi, 1996; Lanza and Siccardi, 1995). As a result, no timely predictions of flooding in the flood prone areas can be performed without relying on quite accurate forecasts of storm areal coverage and related rainfall intensities at least a few hours ahead. Remote sensing technology, and in particular the use of half-hourly IR data from geostationary platforms, allows discrimination of the large scale dynamics of cloud systems still approaching the target region. The main direction and advection velocity of Mesoscale Convective Complexes (MCCs) are detectable from the analysis of sequences of satellite images and the results are extremely useful within the framework of probabilistic procedures for the assessment of the risk of flooding at the regional scale and the eventual issuing of distributed warnings (Lanza and Siccardi, 1994).

The aim of the present paper is to provide a review of the relevant concepts and issues associated with the use of cloud tracking using IR imagery for flash flood forecasting applications. In Section II a preliminary discussion of the suitability of infrared imagery for quantitative rainfall estimation is presented, and in Section III, a description of the typical dynamical characteristics of high intensity rainstorms in the Mediterranean region is given in order to introduce the analysis of the possible role of cloud tracking within the framework outlined. A review of the state of the art in cloud tracking procedures using images surveyed by different radiometers is provided in Section IV so as to form the basis for the description of methodologies developed within the STORM Project and for the discussion of prediction capabilities as addressed in Section V. Two case studies are presented in Section VI, based on satellite observations of real events, before a critical discussion of the results is given in the conclusions.

The paper describes and discusses a selection of results obtained in the framework of Task 2.4 of the EU Environment Programme project on "Flood Hazard Control by Multisensor Storm Tracking in the Mediterranean Area", code named STORM'93 (Storm Tracking and Observation for Rainfall-Runoff Monitoring). Integration of the results within the outline of the overall project and operational issues related to the integration with different sensors are addressed elsewhere in the companion papers published within the present special issue (see Roth *et al.*, this volume, pp. 23–50 for a detailed overview).

II. THE USE OF INFRARED IMAGERY FOR QUANTITATIVE PRECIPITATION FORECASTS (QPF)

The issuing of reliable Quantitative Precipitation Forecasts (QPFs), useful for flash flood warnings, still remains a major challenge among hydrologists, meteorologists and remote sensing scientists. Over the last 20 years, analysis procedures for satellite images have been proposed in order to perform QPF at the scale of medium to large size catchments. Lengthy reviews of estimation methods were made by Barrett and Martin (1981) and Atlas and Thiele (1981): such methods mostly rely on empirical connections, e.g. the fact that, in the VIS band, clouds with highest values of reflectivity have the highest rainfall probabilities and in parallel, in the IR band, coldest clouds denote more precipitation-prone cloud formations.

The uncertainty of such estimates is quite large as no information about the microphysics of the water phase content of the inner cloud system is detectable from the images. Moreover, the available techniques provide estimates of what

is referred to as the "instantaneous" rainfall at the ground. Due to the uncertainty associated with the indirect methods, these are reliable only at the scale of the cloud aggregates and always require a set of ground-based observations for calibration. Such a calibration is in turn affected by the fact that no areal averaged observation of the precipitation process is available at the ground but only information from a spatial extrapolation of rain-gauge measurements.

As a result, quantitative estimation of rainfall rates at the ground from IR data makes sense only when the large scale investigation of the precipitation process is addressed both in space and time, i.e. when the assessment of monthly to annual precipitation over large regions is concerned for agricultural, climatologic or water balance purposes, or over smaller areas and shorter time periods if surface observations are very sparse. Possible use of IR data for "instantaneous" rainfall estimation in flood forecasting should be limited to cases where the hydrological response of large size catchments is to be predicted for a single section of a river network, the latter being the outlet of the catchment and the sole target of the flood forecast.

The application of techniques for the optimal integration of IR satellite information and rain-gauge measurements for estimating rainfall patterns on the Arno River basin (with an upstream area of about 4000 km^2 in the critical section centred on Florence, in central Italy) was recently presented by La Barbera *et al.* (1995). The proposed integration techniques are based on the definition of a data coherence problem and on the application of mathematical programming methods. Comparisons between the observed hydrographs at the target river section and simulated hydrographs obtained through a distributed rainfall-runoff model, using the estimated rainfall patterns as inputs, are addressed for the parametric tuning of the integration procedure. However, the best results are achieved when the relative weight of the ground-based information is greater than that of the satellite rainfall estimates in the optimization algorithm.

As for QPF, the actual prediction content of remotely sensed information from IR sensors is strongly affected by the spatial and temporal scales of any specific application and seems to be quite low for small size basin hydrology (10–100 km^2). In this case, indeed, the inner variability of the rainfall field at much finer scales than the sensor resolution is the major factor governing the probability of occurrence of flash floods in the different sub-catchments making up the investigated area as a whole.

Quite a different approach, to be addressed when investigating the orographically accentuated regions of the Mediterranean area, is that of exploiting the available information about the observed cloud coverage at the mesoscale in order to derive estimates of the probability of occurrence of heavy rainfall events within the framework of the distributed analysis of the risk of flooding at

the regional scale. This approach was recently proposed by Lanza *et al.* (1993) and Lanza and Siccardi (1994). The use of IR images is essential in this context, both for the identification of convective cloud cover and the tracking of the spatial and temporal evolution of such clouds approaching the target region.

III. THE DYNAMICS OF HIGH INTENSITY RAINSTORMS

A very clear definition of the meteorological formations commonly leading to high intensity rainfall in mid-latitudes is provided by Houze and Hobbs (1982): *"It is quite common for several thunderstorms to be grouped together within a mesoscale complex, which covers an area one or more orders of magnitude greater than that covered by an individual thunderstorm. The storms comprising such a complex typically share a common upper-level cloud shield, which appears very prominently in satellite imagery when the system matures. Maddox (1980) has used this fact to define a mid-latitude Mesoscale Convective Complex (MCC) in terms of the time and space scales of its cirriform cloud top (see Table I), as it appears in satellite data. Fritsch et al. (1981) indicate that the precipitation falling from an MCC at a given time typically covers a continuous area of mesoscale dimensions; that is, the individual thunderstorms are embedded in a larger, mesoscale region of precipitation falling from the cloud shield."*

As for the Mediterranean area, MCCs are usually observed to originate during the Autumn season, along the edges of atmospheric disturbances associated with low pressure centres over north-west Europe. They are driven mainly by the presence of local enhancement factors such as thermal effects or orographic barriers (Llasat *et al.*, 1994a, 1994b; Castelli and Corradini, 1994).

TABLE I: Criteria Used to Identify Mid Latitude Mesoscale Convective Complexes in Infrared Satellite Data*

Physical Characteristics	
Size:	(A) Cloud shield with continuously low infrared temperature $\leq -32°C$ must have an area $\geq$ 100.000 (km^2)
	(B) Interior cold cloud region with temperature $\leq -52°C$ must have an area $\geq$ 50.000 (km^2)
Initiation:	Size definitions (A) and (B) are first satisfied
Duration:	Size definitions (A) and (B) must be met for a period $\geq$ 6 hr
Max extent:	Contiguous cold cloud shield (IR temperature $\leq -32°C$) reaches maximum size
Shape:	Eccentricity (minor axis/major axis) $\geq$ 0.7 at time of maximum extent
Terminate:	Size definitions (A) and (B) no longer defined

*From Maddox (1980)

As an example of the occurrence of a typical MCC over the Mediterranean region, the Meteosat IR image at 1300 GMT of 22 September 1992 (from Lanza and Conti, 1995) is showed in Figure 1. The image has been zoomed over a window from 30°N to 60°N and from 20 °W to 30 °E after being georeferenced and plotted in a latitude-longitude coordinate system; coastlines have also been superimposed. From a qualitative perspective, it is easy to identify in the picture at the synoptic scale an extended low pressure field. The MCC was observed to develop over southern France and later advected towards north-west Italy producing heavy rainfall and disastrous flooding along the coastal regions.

As for the evolution characteristics of this kind of meteorological event, again following Houze and Hobbs (1982) *"the dynamics of the development of the mesoscale circulation of the MCC are not yet well understood; however, some of their aspects may be surmised from existing observations, as well as from mesoscale models and by comparing MCCs with tropical cloud clusters. The initial development is apparently driven by convective heating (which is dominated by release of latent heat in the convective updraft (Houze, 1982)) associated with the embedded thunderstorms."*

The results of the meteorological analysis of the most important high rainfall events in north-eastern Spain observed since 1940 have shown common features which allow the identification of a general synoptic pattern (Llasat and Puigcerver, 1994; Llasat *et al.*, 1994a). In recent years this kind of study has been improved by the use of objective analysis and mesoscale analysis. In the
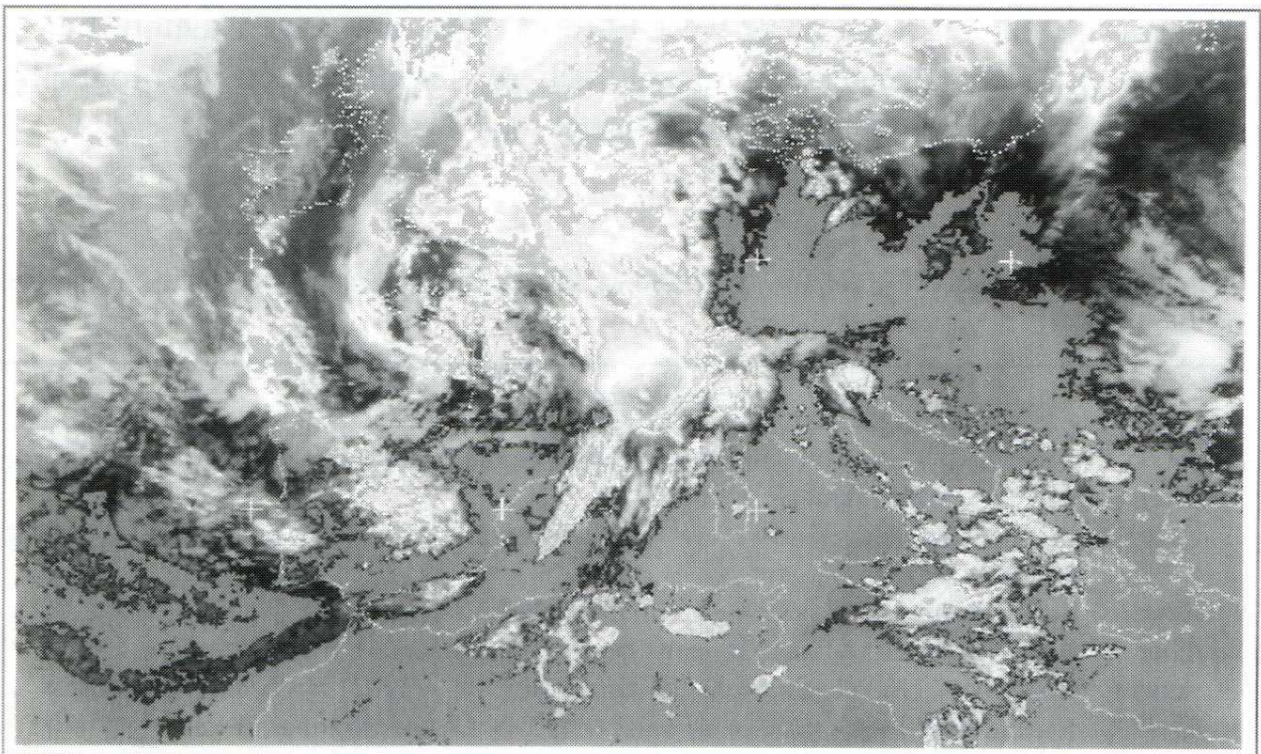

FIGURE 1   Meteosat IR image at 1300 GMT of 22 September 1992 (from Lanza and Conti, 1995). (See Colour Plate XXV at the back of the journal).

first case the location and evolution of the main convective structures is related with key factors, e.g. Convective Available Potential Energy (CAPE), quasi-geostrophic forcing, convergence of water vapor and potential instability, which can be quantified by means of a suitable objective technique (Ramis *et al.*, 1995). The mesoscale analysis provides information about the factors responsible for both the convection localization and triggering mechanisms.

In a recent work, Llasat *et al.* (1994a), use cross-fertilized remotely sensed information and conventional meteorological datasets to identify areas where the main localization and triggering processes took place within the case studies analyzed. The superimposition of meteorological maps and satellite images shows that the occurrence of an MCC is related to the presence of the key factors selected, and to an intense flow which impinges perpendicularly to the coast and the nearest mountain regions. These results reflect the extraordinary role played by the orographic enhancement in triggering convection during the observed events. After the analysis of heavy storms selected from those observed in the last few years over the Mediterranean area, Boni *et al.* (1995) argue that the processing of sequences of satellite images using storm identification and cloud tracking techniques shows a strong interaction between the local orography, the dynamics of the cloud system at the synoptic scale, and the development of convection.

IV. STATE OF THE ART IN CLOUD TRACKING

The concept of cloud tracking relies on the assumption that the areas presenting the highest probability of heavy rainfall within the observed cloud system are actually clustered, so as to reflect the structure of typical MCCs. This means that the pixels showing the lowest values of radiance temperatures in the IR satellite images are aggregated in clearly distinguishable clusters which are easily and automatically identified in each of the images from a sequence, and then tracked, with reference to some suitable cluster characteristics.

Cloud tracking methodologies were, however, developed to be used with different remote sensing information, mainly provided by meteorological radar and geostationary satellites, and aimed at different applications. Cloud tracking using meteorological radar was designed to the real time analysis of rainfall fields associated with warning systems for tornadoes and severe storms. The usefulness of satellite images was originally explored with the aim of detecting cloud motion vectors, assumed to be representative in some way of the wind fields, for meteorological modeling and weather forecasting applications. Most recently

the need for spatially and temporally detailed rainfall forecasts has been pointed out by hydrologists, especially for sewer management and early warnings for flash floods. Several authors proposed the use of meteorological radar data for such purposes (Huff *et al.*, 1980; Bonser and Wong, 1987; Einfalt *et al.*, 1990; Brémaud and Pointin, 1993). This approach is, however, not suitable when flash-flood forecasting for early warnings in the Mediterranean coastal regions of south-west Europe are operationally concerned, for these areas are characterized by small-sized river catchments with very fast responses to the heavy rainfall events (less than one hour). Early warning systems for such regions call for reliable predictions of storm evolution over time intervals of at least the same order of magnitude as that of the population response time to flood warnings (few hours). The synoptic scale investigation of cloud systems, as provided by geostationary satellite images, is needed.

The development of cloud tracking algorithms using sequences of satellite images was addressed by several authors after the first Application Technology Satellite (ATS-I) was launched in 1966. The suitability of the images for measuring cloud displacements was demonstrated early through the analysis of sequences of VIS images, as provided by the Spin Scan Camera System (SSCS) flying on board ATS-I, in a "closed loop" projection. The main idea was that of deriving cloud motion vectors from animated sequences, so as to obtain information about wind speed and direction, to be used as input parameters for numerical weather prediction models.

At first, cloud motion vectors were derived by subjective interpretation of the animated sequences of cloud images through the manual detection of the position of each cloud element at the beginning and at the end of the sequence (Fujita *et al.*, 1968, 1969; Young *et al.*, 1972). It was immediately recognized that such procedures require a large amount of time to process the data, and were not free from operator errors, due to the subjectivity of the method: automation was thus necessary in order to speed up the procedure, using computer capabilities.

Two main methodologies were developed for automated tracking of cloudy areas: cross correlation and the matching of different cloud entities using geometrical features obtained by different methods. Cross correlation techniques were initially addressed as providing the simplest ways to estimate motion vectors of corresponding clouds in two subsequent images. The principle consists of overlying two different images, one observed at time t and another observed at time t + Δt (where Δt is the time interval between two subsequent sampled images) and searching for the 'optimum' shift between the images corresponding to the higher value of the cross-correlation coefficient. The optimal shift is assumed to represent the displacement of the cloud entity in the time interval Δt.

The outline of the procedure detailed below reflects the description of the method as presented by Leese et $al.$ (1971).

The cross-correlation coefficient represents a measure of the relationship between the elements of two different sets of quantities. The two-dimensional cross-correlation is calculated for different lag values between the elements of two input matrices M_t and $M_{t+\Delta t}$ (namely two matrices of grey scale values representing two subsequent satellite images).

The value at generic lag (i,j) is given by:

$$R(i,j) = \frac{Cov(i,j)}{\sigma_t \sigma_{t+\Delta t}}$$

where:

i,j are the lag values in terms of columns and rows of the input matrices respectively;

R(i,j) is the sample cross-correlation at lags i and j;

Cov(i,j) is the sample covariance at lags p and q;

σ_t and $\sigma_{t+\Delta t}$ are the sample standard deviations of the input arrays M_t and $M_{t+\Delta t}$. The coefficients are calculated for values of i and j between the limits:

$-I \leq i \leq I$

$-J \leq j \leq J$

obtaining a matrix of values of $[R(i,j)]_{j=-J,J}^{i=-I,I}$.

The displacement vector of the cloud entities from one image to the subsequent one is proportional to the location of the maximum correlation coefficient. Let i^- and j^- the lag values so that:

$$R(i^-,j^-) = max[R(i,j)]$$

and the speed and direction of the cloud are given by:

$$|V| = \frac{[(i^- \Delta x)^2 + (j^- \Delta y)^2]^{\frac{1}{2}}}{\Delta t}$$

$$\theta = \arctan\left(\frac{i^- \Delta x}{j^- \Delta y}\right)$$

where:

$|V|$ is the speed of the cloud;
θ is the direction (angle between the motion vector and the j direction);
x and y the spatial sampling intervals of columns and rows in the input picture matrix;
Δt the sampling time interval of the input matrices.

These equations can be easily implemented within a computer procedure to calculate automatically cloud motion vectors.

A cross-correlation technique using fast Fourier Transform (FFT) to track cloud entities within ATS-I images was described by Leese *et al.* (1970, 1971) and implemented by Bradford *et al.* (1972). The application of FFT was used to speed up the computation in order to attain suitable procedures for use in a real time operational system. The method aimed at the estimation of low-level wind fields. However, the results showed that the method was not able to discriminate between clouds at different levels and performed bad estimations where high-level cloud layers were present.

Several authors agree in observing that this method is the simplest and the least expensive in terms of calculation load, but it is not suitable in the case of cloud entities presenting rotation, different motions and significant changes in size and shape, since it basically translates the whole cloud field. For frontal storms which present a low degree of differential movement these problems may be negligible but this is not the case when the development of convective activity due to local orography or thermal effects is concerned (Brémaud and Pointin, 1993; Bonser and Wong, 1987). Current research is directed toward methods that can take into account the motion features of the cloud systems at different scales. These methods perform thresholding of the images with selected values (i.e. fixed radiance temperature values for satellite images in the IR band) and singling-out potentially hazardous areas within contour boundaries. These areas are then tracked, performing a match of them between subsequent images (Kumar and Foufoula-Georgiou, 1990). This 'matching' approach has the advantage that different cloud entities can be detected and tracked differently within the same sequence of images. Another advantage is that the individual cloud areas can be analyzed, extracting some geometrical features, while they are tracked: this is of particular interest when the real time forecasting of severe storm evolution is the main goal of the analysis.

The matching approach has been presented by several authors for the analysis of radar echoes. The first methods used only the position of the echo centroid as the geometrical feature able to describe the cloud entities (Barclay and Wilk,

1970). Further developments involved the use of Fourier series to describe the contours of the cloud entity (Ostlund, 1974). Matching was assumed when the echo centroid of an object in a frame fell within the contour of another object in an adjacent frame. Other techniques were developed to take into account in some way the distribution of the intensities within the tracked objects, i.e. fitting to the object a bivariate Gaussian distribution (Wiggert et al., 1976).

The choice of some "brightness centres" (namely the centroids of cloud entities) to determine cloud motion from sequences of geostationary satellite images was addressed by Endlich et al. (1971) and improved by Wolf et al. (1977) while updating the procedure in order to take into account data from images in the IR band. The matching was performed by computing a fitting function taking into account changes in the geometrical features of the objects between subsequent frames for each pair of centres: the lowest value of the function defines the optimal matching between them.

Bonser and Wong (1987) compared the performance of several matching procedures using different geometrical features and concluded that the best shape descriptor was the mass centroid of the object, probably because "*objects are more likely to have changes in shape and size between frames than they are to have large displacements.*"

In the US an interactive precipitation estimation technique—the Interactive Flash Flood Analysis (IFFA) technique (Clark and Perkins, 1985; Scofield and Oliver, 1977)—is an operational method for the real time prediction of heavy rainfall events of convective origins. This can be assumed to be the only presently operational technique involving cloud tracking algorithms as, following the description by D'Souza et al. (1990), "*the main part of the operational convective precipitation estimation technique is based on a decision tree algorithm in which point rainfall amounts are increased from a base value by empirically derived amounts depending on the presence of a number of meteorological signatures assessed from satellite and conventional data sources including approximately 40 items, such as cloud shape, cloud rate of change, cloud lifetime, low-level inflow, saturated environments and atmospheric moisture, in addition to the original elements of cloud top temperatures, overshooting tops and mergers (Scofield, 1987).*" The high number of the parameters involved shows once again that many techniques lack a deeper physical understanding of the rainfall producing processes and basically rely on empirical connections between easily observable parameters and the associated probability of intense rainfall. Within the STORM project an improved Hierarchical Objective Procedure (HOP) has been developed on the basis of the one supporting the IFFA system since 1987 to define areas of cloud likely to give moderate to high-intensity rainfall over southern and western Europe (Barnett and Cheng, this volume, pp. 119–150).

Cloud tracking techniques able to identify and track such cloud entities at the large mesoscale using IR Meteosat images have been presented by Filice *et al.* (1991a, 1991b) and developed by Lanza *et al.* (1994) and Lanza and Conti (1995) in order to forecast the evolution of the potentially hazardous systems identified within sequences of images, and to couple such predictions with suitable spatial disaggregation models of rainfall fields. Rainfall predictions at finer spatial scales than those of the Meteosat images (7×5 km^2 at middle latitudes) are achieved in this way. Other cloud identification and tracking algorithms were designed by Braccini *et al.* (1991) and Bolla *et al.* (1995).

In the following sub-sections two typical approaches are described, by which two different cloud tracking procedures have been derived within the STORM project: the Contour Filtering Approach and the Shape Parametrization Approach. Applications of the procedures described to the case studies analyzed are presented later in Section VI.

A. The Contour Filtering Approach

The first step in this proposed image processing technique concerns thresholding and relaxation. The goal is that of extracting from a sequence of IR Meteosat images that portion of the cloud coverage characterized by the highest rainfall probability. According to the Griffith and Woodley heuristics (Griffith *et al.*, 1978, Adler *et al.*, 1983), areas with radiance temperatures below a specified threshold are defined as clouds with a particular empirically derived, mean rainfall intensity.

Pre-processing techniques, based on a relaxation method, have been applied in order to improve the robustness of the thresholding procedure and to obtain binary matrices from the original grey scale IR images. Relaxation is intended here as a stochastic process (Rosenfeld and Russel, 1981, Touzani *et al.*, 1988) that allows us to classify image pixels in two separate classes (cloudy pixels and background) by taking into account, together with the single pixel value, the radiance temperature characteristics of the neighbouring pixels. The aim of the procedure is that of reducing the inherent errors involved in simplex pixel classification. The output binary image results from removing the isolated cloudy pixels surrounded by background areas and from filling the small background areas inside large sets of cloudy pixels. The implemented algorithm involves:

- a fixed threshold temperature x is chosen for the observed scenario;
- for a given interval 2d, all pixels with values below (x − d) are classified as cloudy pixels, while pixels with values above (x + d) are classified as background;

- pixels with temperatures ranging between $(x - d, x + d)$ are assigned a probability of being cloudy pixels or background pixels which is iteratively updated using the joint probability derived from neighbouring point properties;
- iterations are performed until the variation of the point probabilities falls within a fixed range, or simply after a predefined number of steps.
- finally, pixels with probabilities of being cloudy greater than 0.5 are classified as cloudy pixels, otherwise they are added to the background.

Cloudy pixels, as identified through the relaxation algorithm, are then clustered into fully connected regions (referred to as 'clusters' in the following). To this aim the binary image is scanned from the upper left corner to the lower right one until some cloudy pixel is encountered. That cloudy pixel necessarily belongs to a cluster border and it is used to initialize an edge follower algorithm that operates according to the Sobel scheme (Sobel, 1978). After the external cluster border is detected, the cluster is classified as cloud if 90% of the inner pixels belong to the cloudy pixels set, and is otherwise discarded. The latter case corresponds to clouds presenting large background areas within the cluster. Experimental results have shown that such cases rarely occur once relaxation has been performed. The identified cluster is then removed from the binary image and the raster scanning is continued until the remaining clusters are all extracted.

Image pre-processing is completed by filtering algorithms, aimed at the smoothing of cluster contours by means of low-pass operators so as to discard unessential detailed information which would demand higher computational loads. The operation is performed over each cluster contour by means of a simple monodimensional investigation mask slid along the cluster boundary. The parameters of the low-pass filter are the mask size and the weight of the central point. In order to have a strong smoothing effect, the weight of the central point should be low and the mask size wide enough so as to keep up just the shape of the edge. The operation is performed on the x and y coordinates of each point along the cloud contour. For instance, by using a mask length of five units and a central weight F, the new value for the coordinate x at the i-th point of the edge ($x_{i,new}$) is given by the following expression:

$$x_{i,new} = \frac{x_{i-2,old} + x_{i-1,old} + F \cdot x_{i,old} + x_{i+1,old} + x_{i+2,old}}{F + 4}$$

An analogous expression is used to obtain the y coordinate. In Figure 2, the cluster contour after image processing is depicted: the contour is smoothed, and the detailed information is lost, while the main edge shape is preserved.

Alternative filtering methods have been implemented using a low-pass frequency filter. In this case the operation is performed by the Discrete Fourier Transform (DFT) in the frequency domain rather than directly in the space domain. Let us suppose we have N samples of a discrete signal x(n) with n = 0,..., N − 1; the k-th value of the DFT of x(n) is:

$$x(k) = \sum_{n=0}^{N-1} x(n)e^{-j\,2\pi\,kn/N} \qquad k = 0,\dots, N-1$$

The signal here is the cluster boundary, where the latter will need to be oversampled if the number of entries is not a power of two (as needed to implement frequency filters). By using the expression above the N entries of the DFT signal are obtained, to be later multiplied by the N entries of the low-pass frequency filter defined as:

$$F(k) = \begin{cases} 1 & 0 \leq k \leq \dfrac{N}{2\beta}(1-\alpha) \\[2mm] \dfrac{1}{2}\left[1 - \sin\left[\dfrac{\pi\beta}{N\alpha}\left(k - \dfrac{N}{2\beta}\right)\right]\right] & \dfrac{N}{2\beta}(1-\alpha) < k < \dfrac{N}{2\beta}(1+\alpha) \\[2mm] 0 & k > \dfrac{N}{2\beta}(1+\alpha) \end{cases}$$
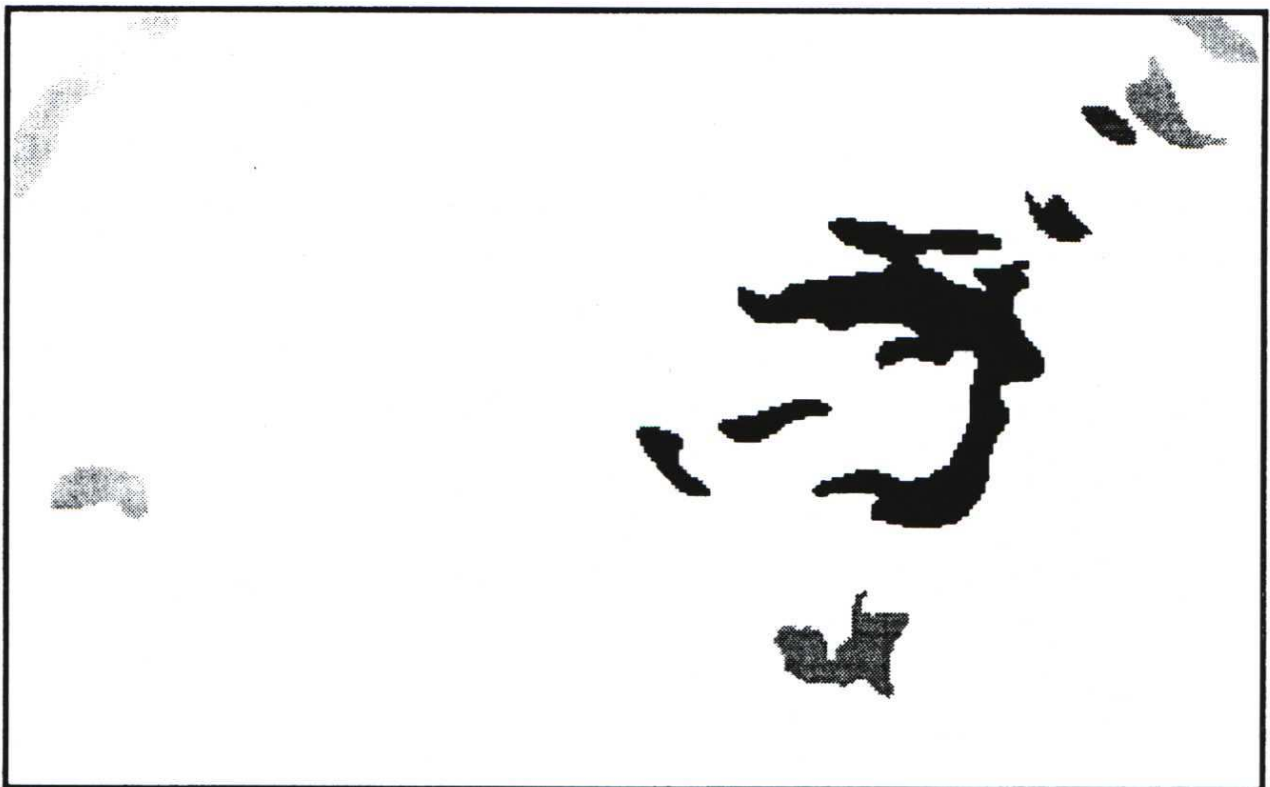
FIGURE 2   Cluster contour obtained after image processing using the contour filtering approach.

where k is in the interval $(0, N - 1)$; β allows for the selection of different cut-off frequencies $N/2\beta$, and α is a classical parameter in low-pass filters. The entries of the product $x(k)F(k)$ are later anti-transformed so as to obtain the filtered boundary coordinates in the space domain. The DFT filter allows us to choose quite accurately the cut-off frequency and the smoothing level of the filter; the same control is much more roughly performed in filtering procedures using masks in the space domain. Figure 3 shows an example of a single filtered cluster, obtained with three different values of β ($\beta = 16$, 64, and 256 corresponding to k values of the cut-off frequency at 32, 8, and 2 respectively) together with the original cluster.

A crucial step is now the identification of corresponding clusters in two subsequent images. A single cluster can change position, orientation, and scale from one image to the next; moreover, it can split, or join other clusters generating totally different cloud formations. The identification of corresponding clusters is performed by three different hypotheses: the case of no splitting and joining, the case of splitting, and the case of joining. In the first case the operation is performed by a variable size rectangle set around the centre of mass of the cluster in the first image and by searching for any centre of mass in the second image still falling inside the given rectangle. If more than one centre of mass satisfies this condition a cost function is evaluated so as to choose the 'best' corresponding cluster. The cost function includes the distance between the centres of mass identified and the variation of cluster areas, in the form:

$$\cos t = B \cdot \sqrt{(x_{b,j} - x_{b,i})^2 + (y_{b,j} - y_{b,i})^2} + A \cdot |Area_j - Area_i|$$

where:

- $x_{b,i}$, $x_{b,j}$, are the x-coordinates of the considered centres of mass in the first and second image, respectively;
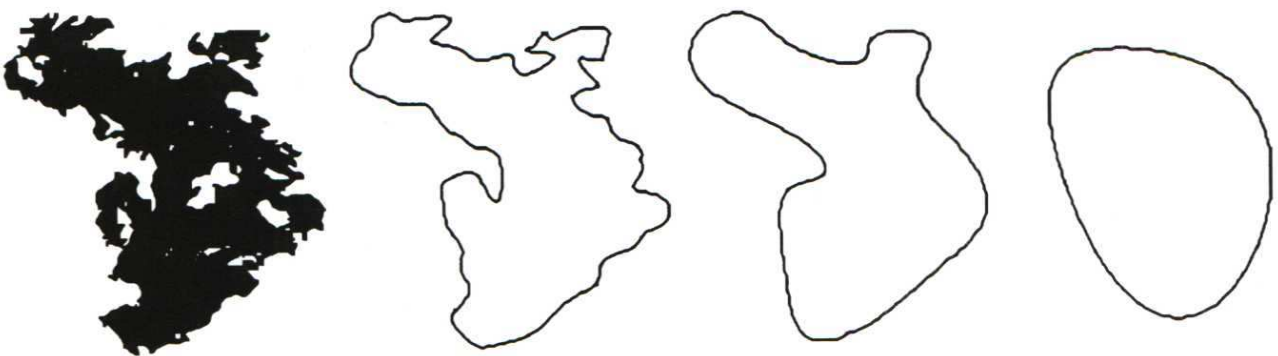
FIGURE 3   Example of a cluster filtered using three different values of ($= 16, 64$ and 256, corresponding to k values of the cut-off frequency at 32, 8 and 2 respectively) together with the original one.

- $y_{b,i}$, $y_{b,j}$ are the y-coordinates of the considered centres of mass in the first and second image, respectively;
- $Area_i$, $Area_j$ are the areas of the considered clusters in the first and second image, respectively.

Each cluster within the first image is analyzed; if any missed cluster exists, the case of possible splitting is investigated. The operation is again performed by setting a rectangle around each cluster in the first image, but now comprising every pixel of the given cluster instead of being set around the centre of mass. Centres of mass in the second image are sought inside the rectangle, and all the possible combinations of those centres are evaluated, selecting the corresponding cluster as the one minimizing the cost function over the permutation process. Once split clusters have been identified, the analysis is directed to the joined clusters; this is performed through an analogous algorithm where the reference rectangle is set on the second image initially.

B. The Shape Parametrization Approach

A much simpler cloud tracking technique based on the shape parametrization approach uses algorithms for cluster analysis as described by Filice *et al.* (1991a) and Filice (1991b); recent developments can be found in Lanza *et al.* (1994) and Lanza and Conti (1995). The images provided half hourly by the Meteosat radiometer in the IR band in the B format have been georeferenced in the latitude-longitude system and the layout of coastlines has been superimposed. A window over the Mediterranean area from 30° to 60° N and from 20° W to 30° E, has been extracted. In view of the clustering process a large amount of data, describing for each image the radiance temperature of clouds at low and middle elevations, is not essential to meet the aim of the analysis. Low and middle elevation clouds are filtered out from the images, by suitable preprocessing, in order to speed up the clustering procedure and to avoid too much noise. Segmentation is performed by means of a fixed threshold, predefined on the basis of the climatological and meteorological characteristics of the area. Processed images then show only the highest level portion of the cloud coverage, namely the one which is associated with the highest probability of heavy rainfall. Usually a threshold at 253°K is set at the middle latitudes for precipitating clouds during the Autumn season even if research is now confirming that fixed thresholds are often too crude to provide best possible results.

Operationally, each pixel x_j in a single IR image (only pixels bounded by a threshold isotherm $T_0 = 253$ °K are considered) is associated with a radiance

value x_{3j}, and two geographical attributes x_{1j}, x_{2j} (Cartesian coordinates). The set of objects to be clustered is represented by vectors:

$$x_j = [x_{1j}, x_{2j}, x_{3j}] \qquad j = 1, ..., n_p$$

where n_p is the number of pixels in each image bounded by the given threshold isotherm. The approach is that of performing a fully automated identification of the main clusters in each image using algorithms belonging to optimization methods, namely the K-mean method (Everitt, 1980; Anderberg, 1973). This simple algorithm consists of the following steps:

(a) begin with any initial configuration of K centroids, or seed points, which act as initial estimates of the cluster centre: a single seed point is used in most cases;

(b) allocate each entry x_j to the cluster with the nearest seed point, where the distance is defined as the geometrical distance in the (x_1, x_2) domain:

$$d(x_j, c_i) = |x_j - c_i| \qquad i = 1, ..., K; j = 1, ..., n_p$$

where c_i is the i-th seed point;

(c) compute new seed point for i-th cluster as the centre of mass of the entries currently in the cluster;

(d) iterate the process till convergence, i.e. continue until no data entries change their cluster membership after the distance test.

The introduction of a reference value d_{lim}, representing the maximum value for acceptable distances, allows us to limit the maximum size of a generic cluster, i.e. pixels with distance exceeding d_{lim} are not accepted in the cluster.

The spatial fragmentation of the identified clusters is tested by comparing the largest of the two principal inertial moments, S_1, with the analogue for a rectangular shape, of characteristics dimensions l_1 and l_2, having the same principal inertial axis, the same mass (number of clustered pixels) and the same skew ratio of the figure associated with the cluster:

$$\sqrt{S_1/S_2} = l_1/l_2 = \alpha$$

with $l_1 \times l_2 = n_i$ (number of pixels of i-th cluster). The fragmentation index:

$$R_f = (l_2 \times l_1^3/12)/S_1$$

gives a measure of cluster compactness. The parameter $R_{f_{lim}}$, introduced as a reference value, represents the maximum degree of fragmentation allowed in the identification procedure. If $R_f > R_{f_{lim}}$ the procedure is stopped, otherwise the characteristic distance d_{lim} is reduced by 10% and the procedure iterated. The identification of each cluster is thus followed by a series of control statements testing its compactness and taking decisions—at each iteration step—upon whether to subdivide it in two independent clusters.

The identification of the possible correspondence between clusters identified in two subsequent images may be done automatically using different techniques. However in this case the analysis is concentrated over a particular region where a potentially hazardous cloud system is identified: often only one cluster develops within that system and if more than one cluster exists, they result from the splitting of the same initial cluster and will be treated, for the aim of the present analysis, as a single object.

V. PREDICTION ALGORITHMS

Aiming at the prediction of the future position of a cluster within the contour filtering approach, some cloud motion model must be assumed. A linear model is proposed so that the movement of each cloudy pixel $\underline{x}_i = (\underline{x}_i, \underline{y}_i)$ can be described as (Charduri and Chatterjee, 1991, Skea *et al.*, 1993):

$$x_i = d + Fx_{i-1}$$

where:

$\underline{x}_{i-1}$ is the position of the pixel at instant $i - 1$;
$\underline{x}_i$ is the position of the pixel at instant i;
$\overline{d}$ is the translation vector;
$\overline{F}$ is the shape matrix.

By using the Polar Decomposition Cauchy theorem, the shape matrix F is written as the product between the two matrices R and U:

$$F = RU$$

with $R \in O^+$ (positive definite) and $U \in Sym$ (symmetrical matrixes). From a physical point of view, the matrix R can be considered as the rotation matrix, i.e. the matrix which contains the information about the rotation angle, q:

$$R = \begin{bmatrix} \cos\theta & \sin\theta \\ -\sin\theta & \cos\theta \end{bmatrix}$$

The matrix U can be interpreted as containing the information about cluster deformation:

$$U = \begin{bmatrix} u_{11} & u_{12} \\ u_{21} & u_{22} \end{bmatrix}$$

with $u_{12} = u_{21}$.

The problem is then reduced to the evaluation of the translation vector $\underline{d}$ and the matrix $F = RU$. The vector $\underline{d}$ is simply computed as the difference between the centres of mass of the cluster in two consecutive frames while the matrix F is evaluated through a minimization algorithm based on not-overlapping surfaces. The estimated parameters associated with the motion and the deformation of the cloud during the transitions between successive frames can be exploited for an efficient prediction of the position and the shape of the cluster in the next frame. The estimation of the parameters of the centre of mass (x_b, y_b), the rotation angle q and the deformation matrix $U = \{u_{11}, u_{12}, u_{21} = u_{12}, u_{22}\}$ are obtained using interpolation functions as available data:

- M previous images in successive instants $(t_0, t_1, \ldots t_{M-1})$
- M values of (x_b, y_b) for each cluster
- M − 1 values of q for each cluster
- M − 1 values of U for each cluster

The succession given by the component of the centre of mass of the cluster is interpolated by a suitable function. Let us consider a number N of functions $p_0(t), \ldots, p_{N-1}(t)$ defined in the interval $(0, M - 1)$: these functions are said to be orthogonal within the given interval if:

$$\sum_{t=0}^{M-1} p_n(t)p_k(t) = 0$$

for every n − k, and:

$$\sum_{t=0}^{M-1} p_n(t)p_k(t) = \|p_n\|^2$$

if $n = k$, where $\|p_n\|^2$ is the Euclidean norm of $p_n(t)$. We can then define an interpolating function $f(t)$ written as a linear combination of $p_0(t),\dots, p_{N-1}(t)$:

$$f(t) = c_0 p_0(t) + c_1 p_1(t) + \dots + c_{N-1} p_{N-1}(t)$$

in which the coefficients $c_0, \dots, c_{N-1}$ are unknown and depend on the set of chosen functions and on the observed parameters. It is easy to demonstrate that:

$$c_n = \frac{\sum_{t=0}^{M-1} f(t) p_n(t)}{\|p_n\|^2}$$

Under the assumption that all the parameters to predict have little variation in time, smooth orthogonal functions, such as polynomials, may be used: this choice offers a further advantage because of the existence of a simple recursive formula to determine the desired number of functions. It can be shown that:

$$p_0(t) = 1$$

$$p_1(t) = t - \frac{M-1}{2}$$

$$\dots$$

$$p_n(t) = p_1(t) p_{n-1}(t) - \frac{\|p_{n-1}\|^2}{\|p_{n-2}\|^2} p_{n-2}(t)$$

If the number M of points in which these functions are defined is equal to the number N of the functions themselves, an exact solution is obtained, i.e. the function $f(t)$ exactly passes through the samples. If M is greater than N an approximate solution is obtained (least squares solution).

As pointed out in the previous paragraphs, what we call 'cluster' is actually an area of cloudy sky characterized by the highest probability of heavy rainfall. On the basis of the assumption that what we identify in the infrared Meteosat images is not a well defined physical entity but rather the result of several different constraints acting on an evolving meteorological scenario, the following consideration of the meaning of the tracking of such an entity is necessary: the traditional approach to the analysis of the dynamics of cloud systems by establishing the correspondence among a selected set of cluster points in two successive images by means of some correlation matrix becomes unsuitable when it is accepted

that no physical correspondence between these points actually exists. Nevertheless some kind of regularity in the successive locations and in the evolution of segmented clusters in the Meteosat images has been recognized.

In the shape parametrization approach the analysis of the evolution in time of some cluster parameters defining a very general shape able to represent the area of highest probability of heavy precipitation in each single image is addressed. The elliptical shape has been chosen in this work because of its simplicity, adaptability and good approximation of the observable cluster shapes. In order to obtain a suitable equivalent elliptical shape the following procedure has been applied:

(a) estimate the mass of the cluster as given by the image processing procedure described in the previous section: this quantity just corresponds to the number of pixels characterized by a brightness temperature above a fixed threshold and belonging to the cluster (the term "mass" must not lead to any confusion, as no estimates of the cloud structure are addressed on the basis of the distribution of the radiance temperatures within the cluster);

(b) estimate the spatial coordinates of the centroid (centre of mass) of the cluster;

(c) estimate the principal inertial moments of the cluster area and the angle formed by the principal axis in the east-west direction;

(d) estimate the principal inertial radius.

The elliptical equivalent shape is defined as the elliptical shape which presents the centre coincident to the cluster centroid, the same direction of the principal axes and the same principal inertial radius. In order to avoid ambiguities with the definition of the rotation angle of the ellipse with respect to the E-W direction, the following criterion has been used: once the rotation angle of a given equivalent ellipse has been defined by the rotation angle of the major (minor) axis, the rotation angle β of the cluster in the following image is the nearest to α, independently of the axis to which it is actually referring. The analysis of results emphasizes that the change of the rotation angle from that corresponding to the major axis to that corresponding to the minor axis, or *vice versa*, takes place only in those cases where the two axes are very similar in length and, being the ellipse very near to a circular shape, the position of the two axes becomes meaningless in practice.

In order to evaluate the potential of tracking the parameters of the elliptical equivalent shape, two different procedures have been used, namely the prediction over a lead time of half an hour and one hour respectively. In the first case the parameters, i.e. the principal axis, rotation angle and location of the centroid, are predicted by a linear auto-regressive procedure on the last four available

images. Forecasting over a lead time of two time steps is performed using a linear autoregressive method on the last three available images and on the parameters derived from the one step forecast as previously obtained. Appropriate filtering has been introduced in order to take account of possible missing images. The analysis of cloud tracking in the parameter space, and the performance of the forecasting procedure, has been carried out on the basis of the two case studies described in the following section.

VI. CASE STUDIES

With the aim of discussing results of the application of the described cloud tracking techniques two specific case studies have been selected from several observed and analyzed during the STORM '93 research activity. In both cases the evolution of the events was quite stable and the main convective structure, identified by the area of coldest cloud top temperatures, was clearly clustered giving a chance for a fruitful application of the cloud tracking techniques described above. The IR images from the Meteosat geostationary platform have been processed thus for both cases in order to define suitable cluster characteristics needed for eventual tracking.

The prediction procedure based on the contour filtering approach has been applied to the sequence of three satellite images shown in Figure 4 for the meteorological scenario observed from 0800 GMT to 0900 GMT of 12 June, 1994. Figures 5 and 6 show the predicted images at one step and two steps forward respectively, together with the cluster actually observed by the satellite for the current time step.

In Figure 7 the path of the observed and predicted rotation angles for the same sequence is plotted versus time; the predicted value is close to the observed one, especially in the one step prediction. The same considerations apply to the analysis of the path of the deformation parameter u_{11}, plotted in Figure 8.

FIGURE 4   Clusters obtained from the sequence of satellite images from 0800 to 0900 GMT of 12 June, 1994.

FIGURE 5   Cluster predicted one step ahead (left) and the actually observed one (right).

It is easily detectable from the inspection of the figures that the shape of the predicted cluster does not differ much from the actual observed shape; even small scale details are preserved and the little differences that can be noted derive from the linear model used to describe the motion and the deformation of a cloud. The utilization of a simplified linear model agrees with the original assumption of cloud tracking, where the timing of the satellite sampling is assumed to be frequent enough to ensure that noticeable abrupt changes in the cluster characteristics are not likely to occur between each image and the subsequent one. The above remarks are, however, limited to the analysis of the single case study and still need to be confirmed through a wider application to a large number of cloud cluster sequences.

From the hydrometeorological perspective the prediction of small scale details could be useless due to the large uncertainties associated with QPF within the predicted cloud coverage. Nevertheless the contour filtering approach can be suitably tuned in order to preserve the requested level of information detail by choosing a proper cut-off frequency during the filtering phase.
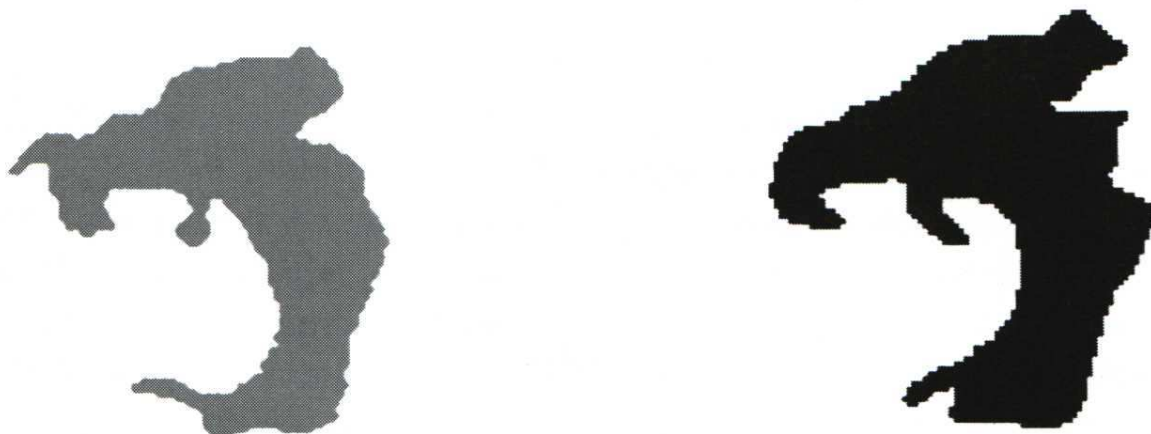
FIGURE 6   Cluster predicted two steps ahead (left) and the actually observed one (right).
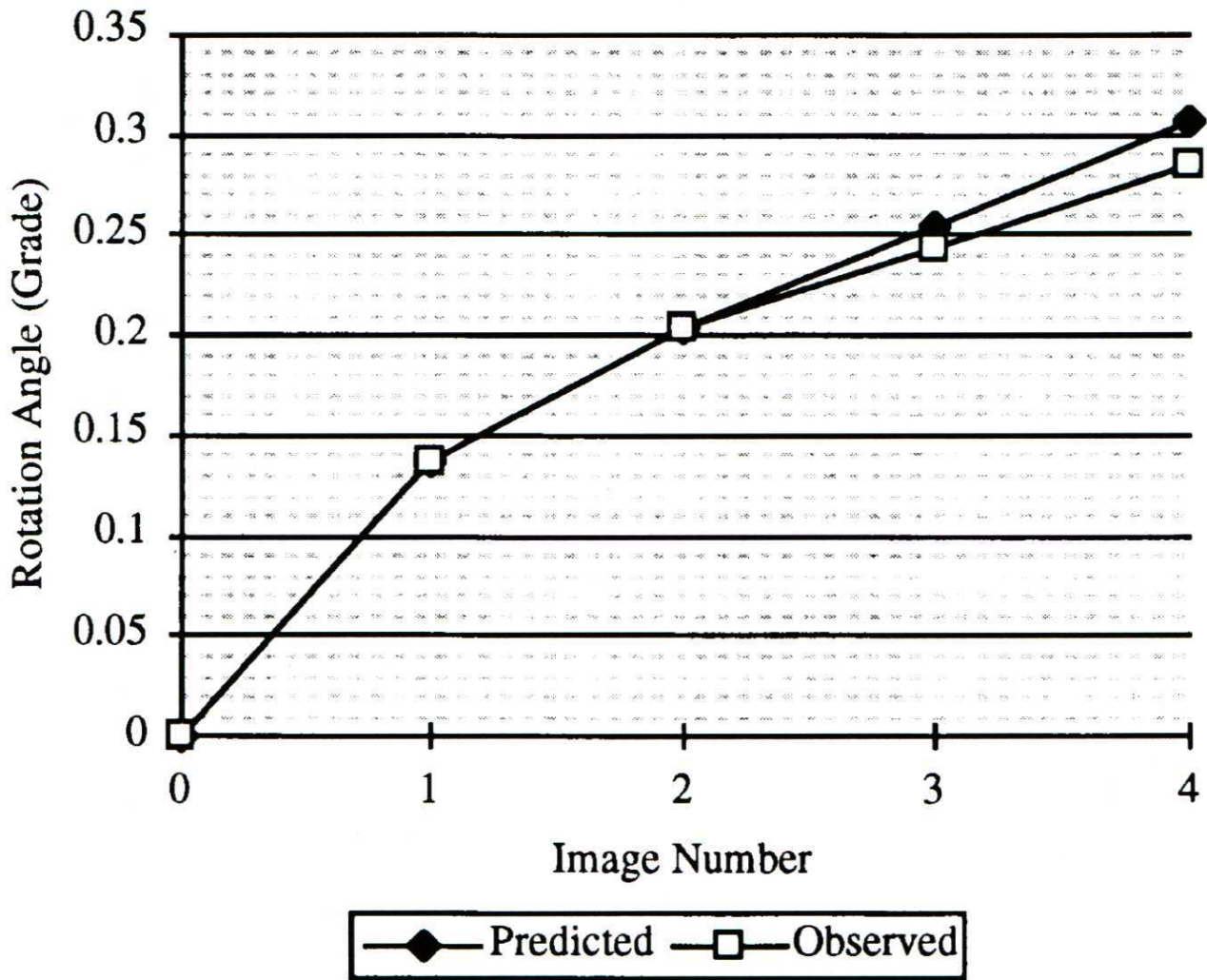
FIGURE 7   Evolution of the observed and predicted rotation angles for the sequence depicted in Figures 4 to 6.

The second case study was investigated using the shape parametrization approach, assuming that small scale details would have to be discarded because they would comprise deterministic constraints with very large uncertainties yet no physical basis if the probabilistic approach to distributed warnings using cloud tracking results as proposed by Lanza and Siccardi (1994) was followed. Heavy rainfall occurred on 27 and 28 September 1992 over the northern Mediterranean area and was responsible for the occurrence of flooding within the urban area of the city of Genova, Italy and the nearby catchments. The MCC originated in this case over southern France as the result of the presence of a large atmospheric low extending from the Bay of Biscay to the Balearic Islands. This had an associated major frontal system moving rapidly towards the east. The Liguria region of Italy was covered by the main convective structure from the morning of 27 September to the morning of 28 September. The core of the event was later located over the Tyrrhenian Sea and the convective cell reached southern Italy before definitive dissolution. A sample from the sequence of half-
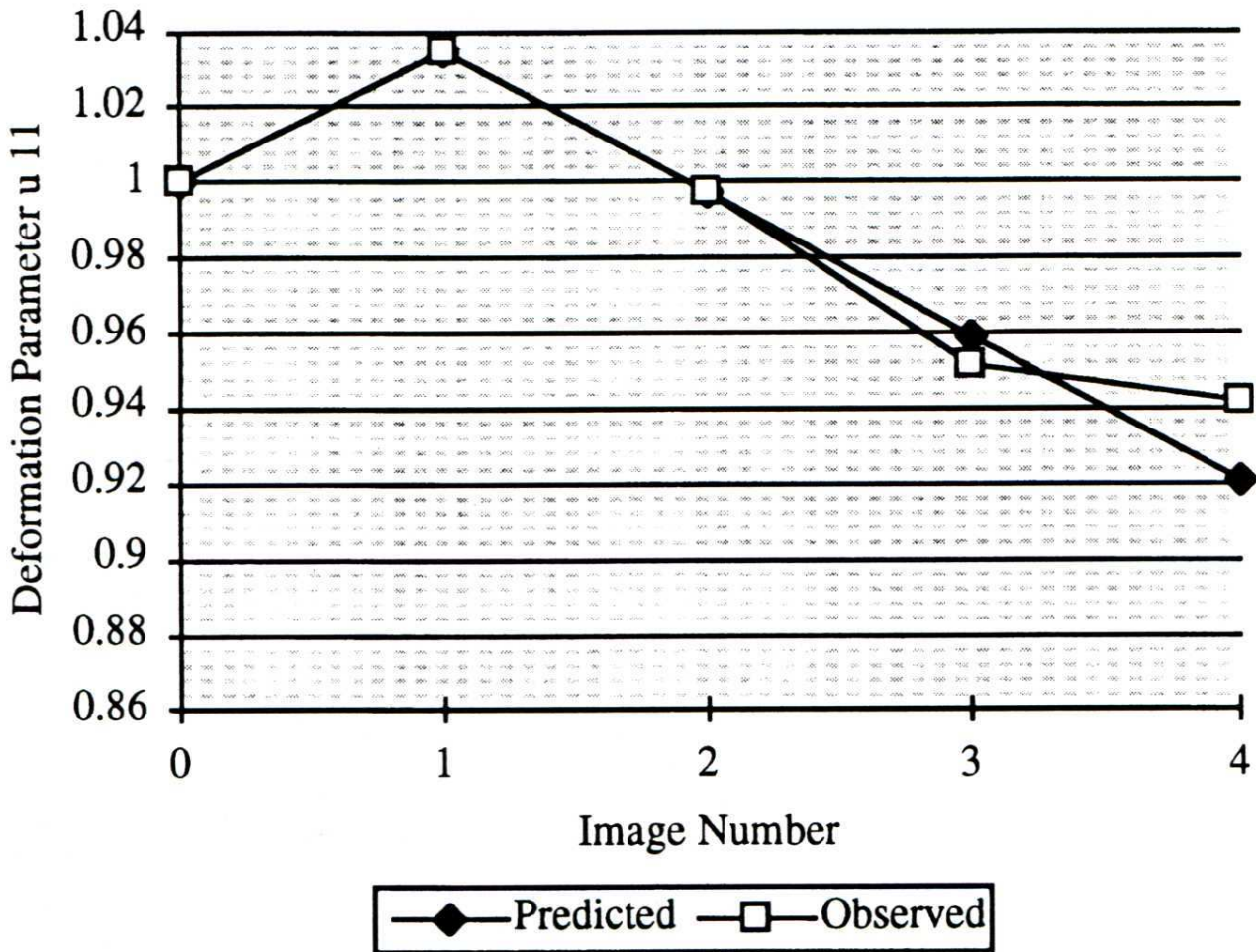
FIGURE 8   Evolution of the observed and predicted deformation parameter u_{11} for the sequence depicted in Figures 4 to 6.

hourly Meteosat images in the IR band for this event is shown in Figures 9a, b, together with the isolated clusters, from 1900 GMT to 2300 GMT of 27 September 1992.

The output of the cloud tracking procedure is summarized in Figures 10a and b. Note that, in Figure 10a, the centre of mass shows a quite irregular path compared with the quite stable evolution of the whole system. This is due to the physical nature of the entity we are actually tracking, for in each image the cluster is a different object with a quite independent shape and areal coverage. The observed path is thus the result of the superposition of two main atmospheric components: the overall dynamics of the system (quite stable in both cases) and the variability of the location of the centre of mass which is mainly a function of the modifications in shape. This is easily detectable by comparing the graphs in Figures 10a and b: the most significant changes in the location of the centre of mass correspond to the largest variations in the cluster areal coverage. The high variability in shape is due to the growth or dissolution of different small scale formations within the cluster, resulting from the turbulent nature of the convection mechanisms which have generated the cluster as observed by the satellite sensor.
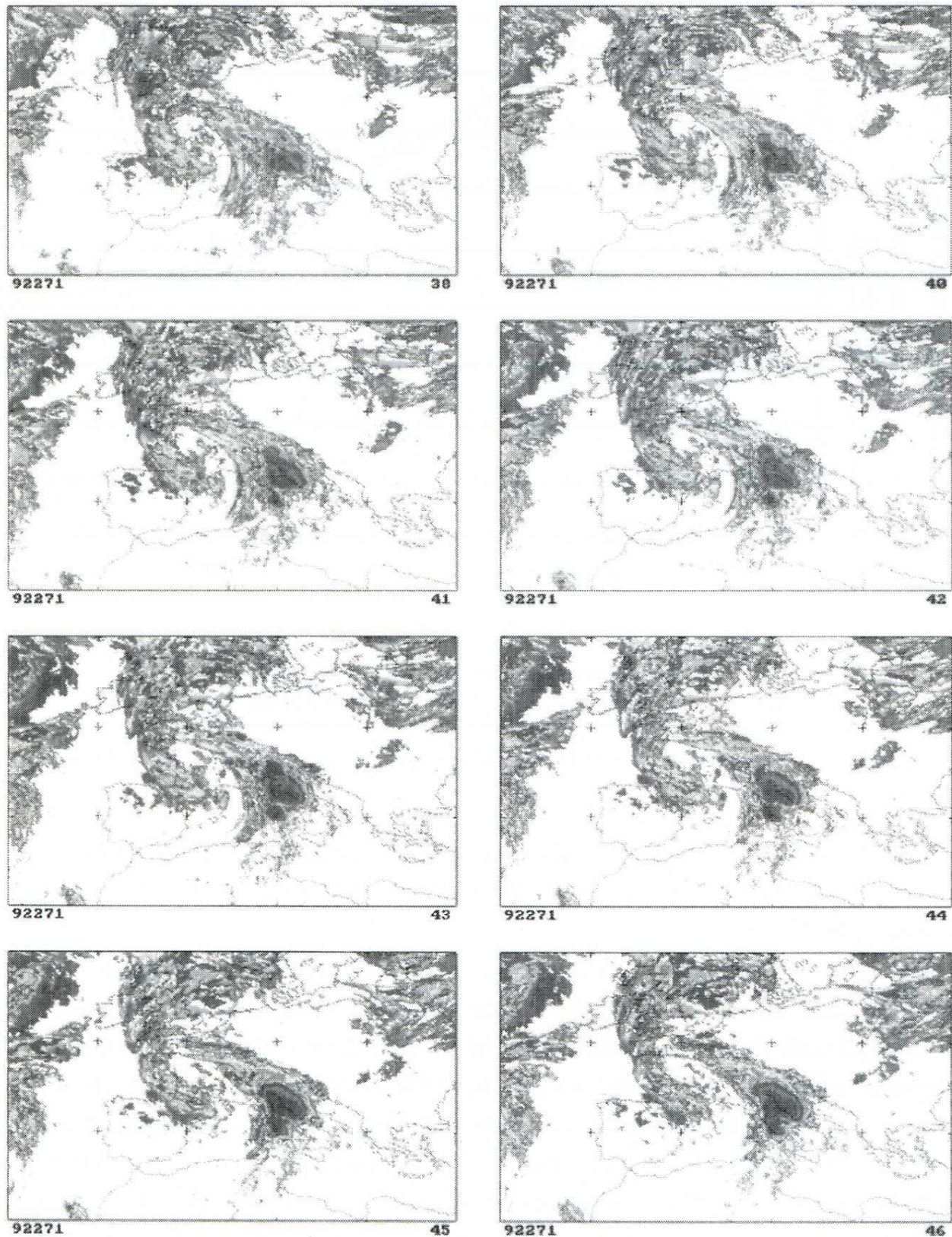
FIGURE 9a   Sequence of half-hourly Meteosat images in the IR band from 1900 GMT to 2300 GMT of 27 September 1992. (See Colour Plate XXVI at the back of the journal).

By analyzing the evolution path of the main cluster in relation to the outline of the orographic barrier in the region (the Apennines), rising almost parallel to the Italian coastline of the Tyrrhenian Sea, it appears quite evident that the evolution itself is strongly driven by the orography. Such a qualitative observation is confirmed by the graph of Figure 11 (from Conti *et al.* 1994), where the
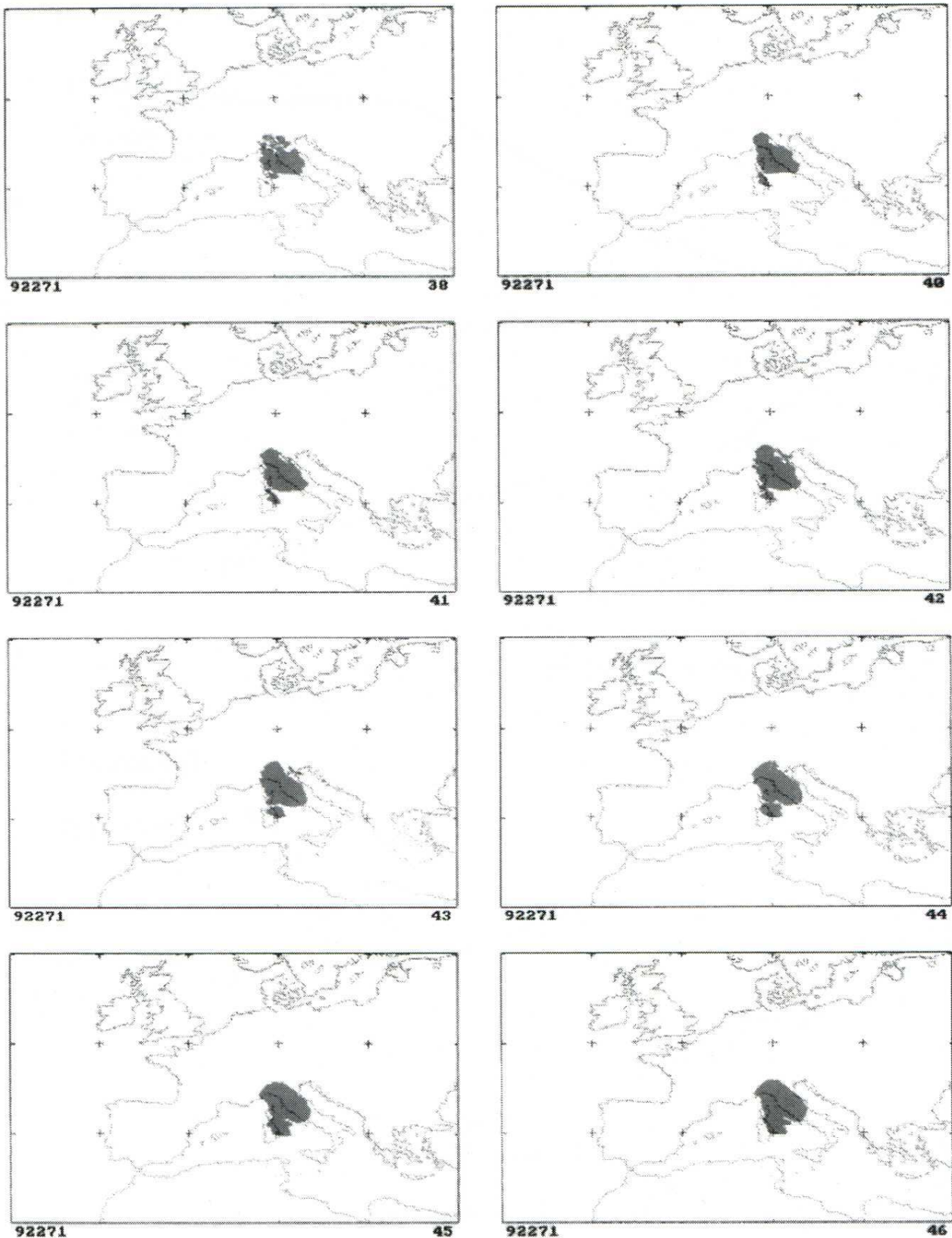
FIGURE 9b   Cluster identification for the sequence of half-hourly Meteosat images in the IR band from 1900 GMT to 2300 GMT of 27 September 1992. (See Colour Plate XXVII at the back of the journal).

path of the cluster centroid in the second event is plotted in a latitude-longitude coordinate system, together with the outline of the main orographic barrier in the region.

a) evolution in time of the centre of mass.

b) evolution in time of the cluster area.
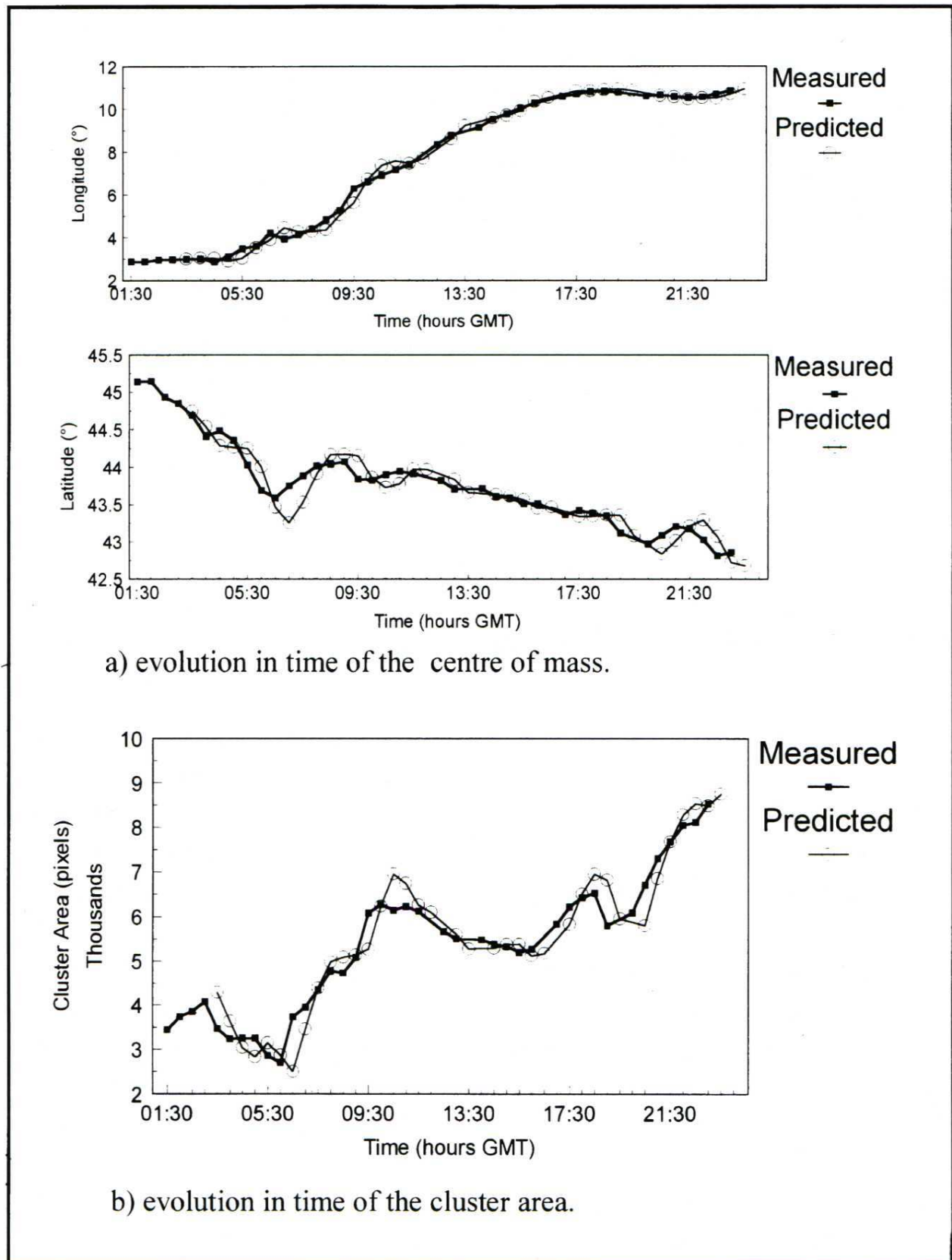
FIGURE 10   Evolution in time of the cluster in terms of path of the centre of mass (a) and path of the number of clustered pixels (b) and predictions at one step in advance from 0130 GMT to 2330 GMT of 27 September.

VII. CONCLUSIONS

A degree of caution should be placed on the interpretation of the results of the cloud tracking procedures presented above, as the technique involved has no
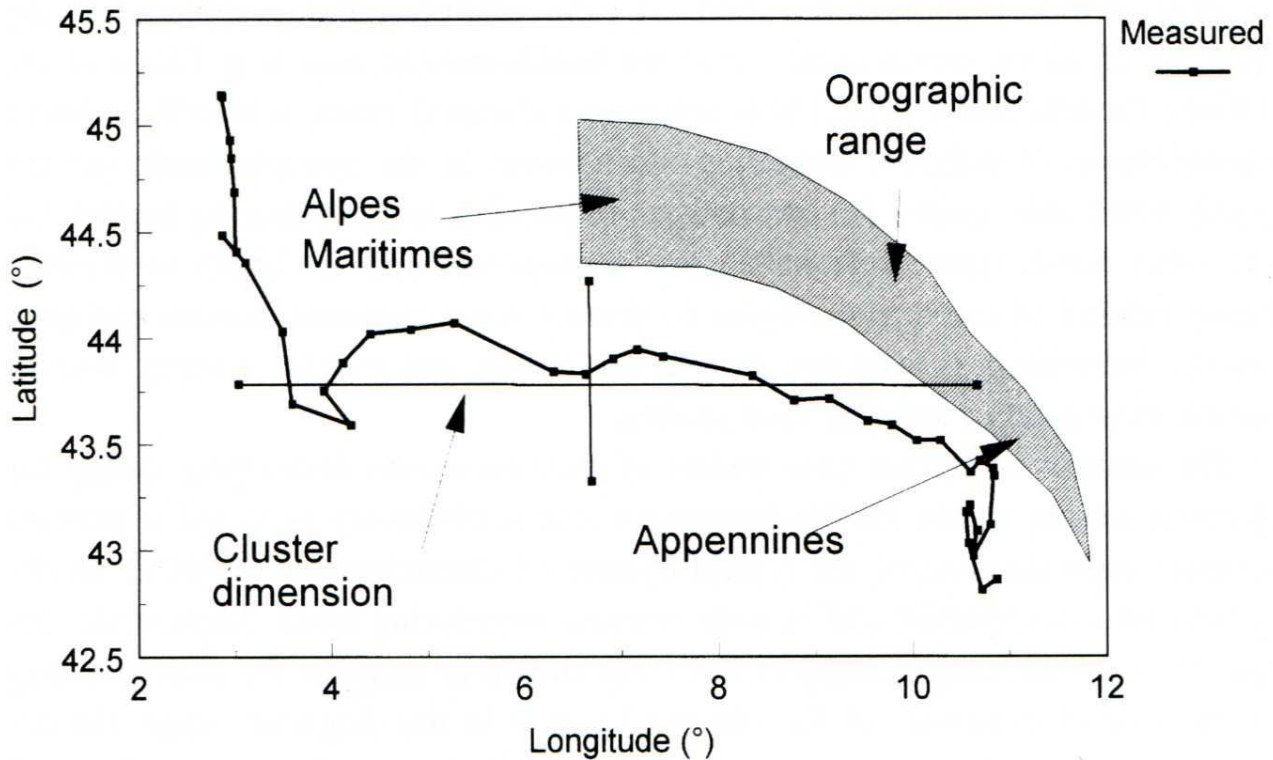
FIGURE 11 Evolution of the main cluster-path of the centre of mass and outline of the main orographic barrier (from Conti *et al.* 1994).

physical basis: the "entity" which is tracked is not actually an individual cloud moving in space from one image to the subsequent one. In fact, in the case of MCCs, the observed coldest top of the cloud system is the result of some convective activity originated by the interaction between several meteorological forcing factors which are not taken into account by any presently available cloud tracking procedure.

Though relying essentially on image processing techniques, the approach of cloud tracking using satellite data seems quite useful for the short term prediction of the dynamics of MCCs because the resolution scale of the temporal sampling provided by the satellite sensor is short enough to ensure that noticeable abrupt changes in the cluster characteristics are not likely to occur between two subsequent images.

However, the operational application of storm identification and cloud tracking techniques is strongly affected by the need for a better physical understanding of the processes involved. The next step in the development of satellite based prediction procedures is that of conceptually and operationally coupling the image processing component with some meteorological model able to convey the extrapolation of the observed cluster behavior towards the most probable mesoscale scenario. For this, traditional meteorological observations would be needed in real time at a suitable resolution. Certainly influence of local enhancing factors (e.g. orography and thermal anomalies) is significant in driving the dynamics of the cloud entities at the mesoscale.

Most of the available applications of some interdisciplinary approach to the analysis of severe storm events over the Mediterranean area (e.g. Llasat *et al.*, 1994b; Castelli and Lanza, 1994) relate to individual cases, where the relative contributions of different triggering mechanisms at the synoptic scale are not easily detectable against the contribution of possible local enhancing factors. On the other hand, typical meteorological scenarios which are likely to produce heavy rainfall of convective origins do present some common features and quite similar behaviours (Llasat and Puigcerver, 1994), and call for a larger investigation over a set of suitable case studies.

The analysis of further case studies of extreme events developing during the Autumn season within the Mediterranean area is obviously expected to provide a better understanding of the typical dynamical characteristics of MCCs as observed by conventional and remote sensing monitoring tools. Meanwhile, the use of cloud tracking techniques has been shown to increase the understanding of the overall dynamics of the observed events in the diagnosis stage: the development of prediction techniques based on such improved understanding will possibly lead to a wider use of IR satellite imagery for prognosis, especially in operational flash flood forecasting applications.

Acknowledgements

References

Adler, R.F., Negri, A.J., Wetzel, P.J. (1983): Rain estimation from satellite: an examination of the Griffith-Woodly technique, *Journal of Climate and Applied Meteorology*, Vol. **23**.

Anderberg, M.R. (1973): *Cluster Analysis for Applications*. Academic Press. New York.

Atlas, D. and Thiele, O.W. (1981): *Precipitation Measurements from Space*. Workshop rep. DI54-8 NASA, Greenbelt MA.

Barclay, P.A., Wilk, K.E. (1970): Severe thunderstorm radar echo motion and related weather events hazardous to aviation operators. *ESSA Technical Memorandum* ERLTM-NSSL 46. National Severe Storm Lab., Norman, Oklahoma.

Barrett E.C., and Martin, D.W. (1981): *The Use of Satellite Data in Rainfall Monitoring*, Academic Press, London.

Bolla, R., Marchese, M., Nobile, C., and Zappatore, S. (1995): Prediction of short term evolution of cloud formations based on Meteosat image sequencies, *Proceedings of the International Conference on Image Analysis and Proceedures* (ICIAP'95), Sanremo, Italy, Sept. 95.

Boni, G., Lanza, L. and Conti, M. (1995): Tracking storms using satellite images: the role of the orography and a few comments. (*Abstract*) *Annales Geophysicae* **13**, Suppl. I, (C-206) XX General Assembly of EGS, Hamburg, Germany, 3–7 April 1995.

Bonser, J.D. and Wong A.K.C. (1987): A feature based method for tracking mesoscale rainfall areas in radar images. *Stochastic Hydrology and Hydraulics*, **1**, 185–198.

Braccini, C., Gambardella, G., Grattarola, A., Lavagetto, F., Zappatore, S. (1991): Estimating cloud formation evolution from sequences of Meteosat images, *Proceedings of the International Conference on Digital Signal Processing*, V. Cappellini and A. G. Constantinides eds., Elsevier, Amsterdam, 1991, 585–590.

Bradford R., Leese, J. and Novak, C. (1972): An experimental model for the automated detection, measurement and quality control of low-level cloud motion vectors from geosynchronous satellite data. *Proceedings of the 8th International Symposium on Remote Sensing of the Environment*, 441–451

Brémaud, P.J. and Pointin Y.B. (1993): Forecasting heavy rainfall from rain cell motion using radar data. *Journal of Hydrology*, **142**, 373–389.

Castelli, F. and Corradini, C. (1994): A semigeostrophic model for the diagnosis of frontal precipitation over complex orography. *Proceedings of the International Conference on Atmospheric Physics and Dynamics in the Analysis and Prognosis of Precipitation Fields*, Rome, 15–18 November 1994, 270–294.

Castelli, F. and Lanza, L. (1994): Scales of predictability of heavy rainfall events: a case study for the Mediterranean area. *Proceedings of the International Conference on Atmospheric Physics and Dynamics in the Analysis and Prognosis of Precipitation Fields'*, Rome, 15–18 November 1994, 198–202.

Chadhuri, S. and S. Chatterjee (1991): Motion analysis of a homogeneously deformable object using subset correspondences. *Pattern Recognition*, **24(8)**, 739–745.

Clark, D. and Perkins, M. (1985): The NOAA Interactive Flash Flood Analyzer. In *Preprints, International Conference on Interactive Information and Processing Systems for Meteorology, Oceanography and Hydrology*, Boston, Mass., American Meteorological Society, 255–259.

Conti, M. Lanza, L. and Siccardi, F. (1994): predictability of heavy rainfall patterns over the southern european regions. STORM '93 and GNDCI recent research experiences. *Proceedings of International Works on Flood and Inundations Related to Large Earth Movements*, Trento, Italy, October 4–7, 1994. In press.

D'Souza, G., Barrett, E.C. and Power, C.H. (1990): Satellite rainfall estimation techniques using visible and infrared imagery. *Remote Sensing Reviews* **4(2)**, 379–414.

Einfalt, T., Denoeux, T. and Jacquet, G. (1990): A radar rainfall forecasting method designed for hydrological purposes. *Journal of Hydrology*, **114**, 229–244.

Endlich, R.M., Wolf, D.E., Hall, D.J. and Brain, A.E. (1971): Use of a pattern recognition technique for determining cloud motions from sequences of satellite photographs. *Journal of Applied Meteorology*, **10**, 105–117.

Everitt, B. (1980): *Cluster Analysis*. Halsted Press, Div. John Wiley, New York.

Filice, E., La Barbera, P. and F. Siccardi, (1991a): Cluster analysis in the identification of clouds patterns. *Proceedings of X IASTED International Conference on Modeling, Identification and Control*, Innsbruck, Austria, February 18–21, 311–314.

Filice, E., La Barbera, P. and F. Siccardi, (1991b): Cloud entities identification from Meteosat images using cluster analysis. (*Abstract*). EGS XVI General Assembly, Wiesbaden, Germany, April 22–26, 1991.

Fritsch, J.M., Maddox, R.A. and Barnston, A.G. (1981): The character of mesoscale convective complex precipitation and its contribution to warm season rainfall in the U.S. Preparatory Conference on Hydrometeorology, 1981. pp. 94–99.

Fujita, T., Bradbury, D.L., Murino, C. and Hull, L. (1968): *A Study of Mesoscale Cloud Motions Computed from ATS-I and Terrestrial Photographs*. SMRP Research Paper 71, University of Chicago, 25 pp.

Fujita, T., Watanabe, K. and Izawa, T. (1969): Formation and structure of anticyclones caused by large-scale cross equatorial flows determined by ATS-I photographs. *Journal of Applied Meteorology*, **8**, 649–667.

Griffith, G.C., Woodley, D.N., Grube, P.G., Martin, D.W., Stout, J.E., Sidkar, D.N. (1978): Rain Estimation from Geosynchronous Satellite Imagery—visible and Infrared Studies. *Monthly Weather Review* 106, 1153–1191.

Houze, R.A.Jr. (1982): Cloud clusters and large-scale vertical motion in the tropics. *Journal of the Meteorological Society of Japan* **60**, 396–410.

Houze, R.A. and Hobbs, P.V. (1982): Organization and structure of precipitation cloud systems. In: Saltzman (ed) *Advances in Geophysics*. Academic Press. 225–315.

Huff, F.A., Chagnon, S.A., and Vogel, J.L. (1980): Convective rain monitoring and forecasting system for an urban area. *Proceedings of the 19th Conference on Radar Meteorology*, 26–29 Oct. 1976, Miami, American Meteorological Society, Boston, MA, 526–532.

Kumar, P. and Foufoula-Georgiou E. (1990): Fourier domain shape analysis methods: a brief review and an illustrative application to rainfall area evolution. *Water Resources Research*, **9**, 2219–2227.

La Barbera, P., Lo Casto, S., Minciardi, R. and Paolucci, M. (1995): Integrating Meteosat satellite and rain-gauge information to estimate rainfall patterns. *Surveys in Geophysics.* **16(2)**, 183–199.

Lanza, L., La Barbera, P. and Siccardi, F. (1993): Early warnings and quantitative precipitation forecasting. In: Rossi, Harmancioglou and Yevjevich (eds) *Coping with Floods*. NATO-ASI Series, Kluwer Academic Publishers, Dordrecht, The Netherlands. pp. 413–435.

Lanza, L. and Conti, M. (1995): Cloud tracking using satellite data for predicting the probability of heavy rainfall events in the Mediterranean area. *Surveys in Geophysics.* **16(2)**, 163–181

Lanza, L., Conti, M. and Boni, G. (1994): The role of cloud tracking techniques in the short term prediction of flood hazard at the regional scale. *Proceedings International Workshop on Climate Change and Hydrogeological Hazards in the Mediterranean Area*. Colombella (Perugia), 27–28 June 1994, 167–180.

Lanza, L. and Siccardi, F. (1994): Distributed warnings. In: Rosso, Peano, Becchi and Bemporad (eds) *Advances in Distributed Hydrology*, Water Resources Publications. 293–306.

Lanza, L. and Siccardi, F. (1995): Hydrometeorological hazard in a changing perspective. *Surveys in Geophysics* **16(2)**, 137–139.

Leese, J.A., Novak, C.S., Taylor, V.R. (1970): The determination of cloud pattern motions from geosyncronous satellite image data. *Pattern Recognition*, **2**, 279–292.

Leese, J.A., Novak, C.S., Clark, B.B. (1971): An automated technique for obtaining cloud motion from geosyncronous satellite data using cross correlation. *Journal of Applied Meteorology*, **10**, 118–132.

Llasat, M.C. and Puigcerver, M. (1994): Meteorological factors associated with floods in the North-Eastern part of the Iberian Peninsula. *Natural Hazards* **9**, 81–93.

Llasat, M.C., Lanza, L., Barrantes, J. and Boni, G. (1994a): A systematic approach to the analysis of severe-storm events using multisensor information. *Proceedings of the International Conference on Atmospheric Physics and Dynamics in the Analysis and Prognosis of Precipitation Fields*, Rome, 15–18 November 1994, 47–50.

Llasat, M.C., Barrantes, J., Lanza, L. and Ramis, C. (1994b): Predictive potential of joint cloud tracking techniques and meteorological analysis oriented to flash flood forecasting. (Abstract) XIX Gen. Ass. of EGS, Grenoble, France, 25–29 April 1994. *Annales Geophysicae* **12**, Suppl. II, C-440.

Maddox, R.A. (1980): Mesoscale convective complexes. *Bulletin of the American Meteorological Society* **61**, 1374–1387.

Mason, B.D. (1981): Meteosat—Europe's contribution to the global weather observing system. In: A.P. Cracknell (ed) *Remote Sensing in Meteorology, Oceanography and Hydrology*. John Wiley, Chichester, UK. 56–65.

Ostlund, S.S. (1974): Computer Software for Rainfall Analyses and Echo Tracking of Digitized Radar Data. *NOAA Technical Memorandum*, ERL WMPO-15.

Ramis, C., Alonso, S. and Llasat, M.C. (1995): A comparative study between two cases of extreme rainfall events in Catalonia. *Surveys in Geophysics.* vol. **16(2)**, 141–161.

Rosenfeld, A. and Russel C. Smith (1981): Thresholding using Relaxation. *IEEE Transactions on Pattern Analysis and Machine Intelligence* Vol. P.A.M.I. **3(5)**, 588–606.

Roth, G., Barrett, E., Guili, T., Goddard, J., Llasat, M., Minciardi, R., Magnai, A., Scartilli, G., Siccardi, F. (1996): Flood hazard control by multisensor storm tracking in the Mediterranean area *Remote Sensing Reviews*. This Issue, pp. 23–50.

Scofield, R.A. (1987): The NESDIS operational convection precipitation estimation technique. *Monthly Weather Review* **115**, 1773–1792.

Scofield, R.A. and Oliver, V.J. (1977): A Scheme for Estimating Convective Rainfall from Satellite Imagery. *NOAA Technical Memorandum*, NESS 86, Washington D.C., 47 pp.

Siccardi, F. (1996): Rainstorm hazards and related disasters in the western Mediterranean region. *Remote Sensing Reviews*. This Issue, pp. 5–21.

Skea, D., Barrodale, I., Kuwahara, R., and Poeckert R. (1993): A control point matching algorithm. *Pattern Recognition*, **26**, 2, 269–276.

Sobel, I. (1978): Neighborhood coding of binary images for fast contour following and general binary array processing, *Computer Graphics Image Processing*, **8**, 127–135.

Touzani, A., J.G. Postaire (1988): Mode detection by Relaxation, *IEEE Transactions on Pattern Analysis and Machine Intelligence* **10**, 6, 970–978.

Young, M.T., Doolittle, R.C. and Mace, L.M. (1972): Operational Procedures for Estimating Wind Vectors from Geostationary Satellite Data. *NOAA Technical Memorandum* NESS-39, NOAA.

Wiggert, V., Ostlund, S.S., Lockett, G.J., Stewart, J.V. (1976): Computer Software for the Assessment of Growth Histories of Weather Radar Echoes. *NOAA Technical Memorandum*, ERL WMPO-35.

Wolf, D.E., Hall, J.D. and Endlich, R.M. (1977): Experiments in automatic cloud tracking using SMS-GOES data. *Journal of Applied Meteorology*, **16**, 1219–1230.
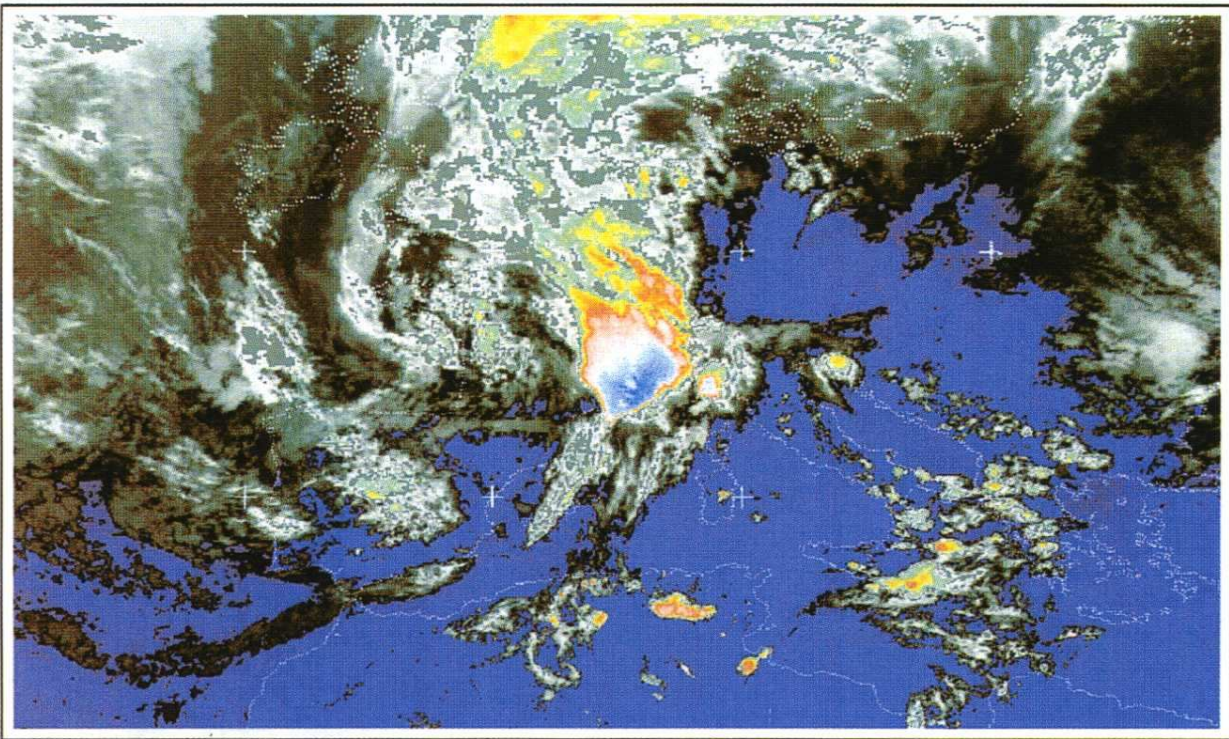
COLOUR PLATE XXV

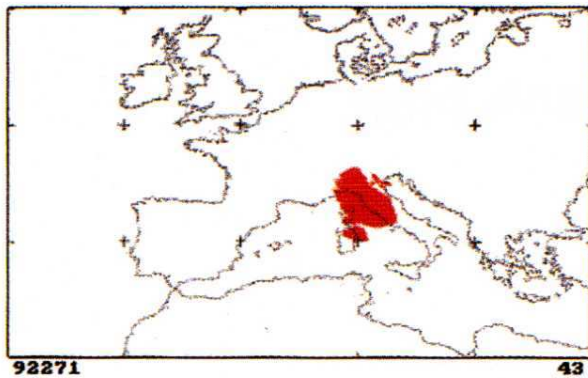FIGURE 1   Meteosat IR image at 1300 GMT of 22 September 1992 (from Lanza and Conti, 1995).
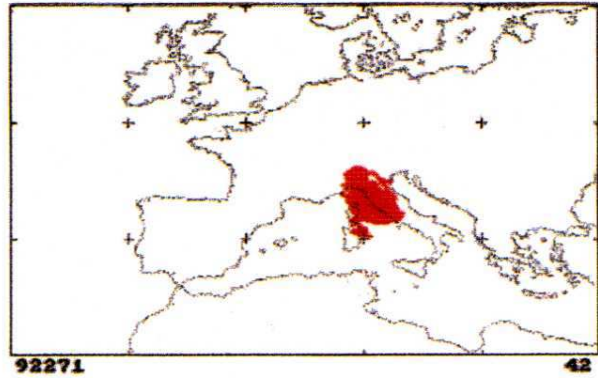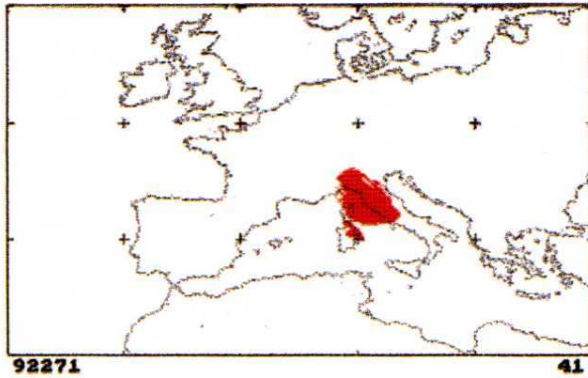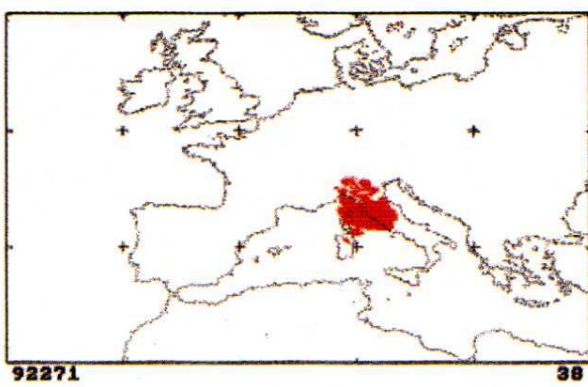(See page 156).
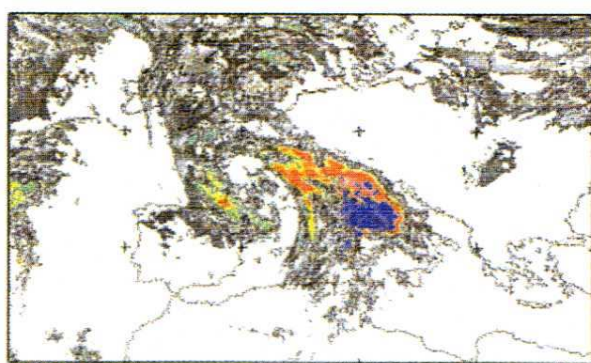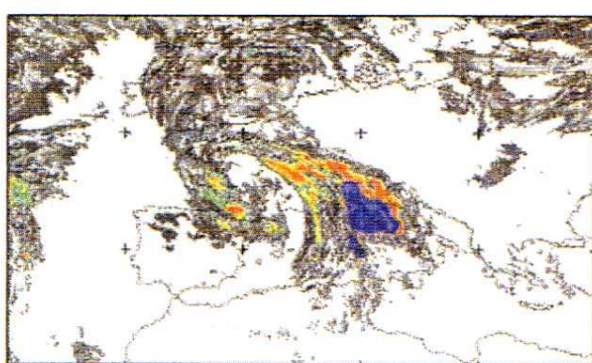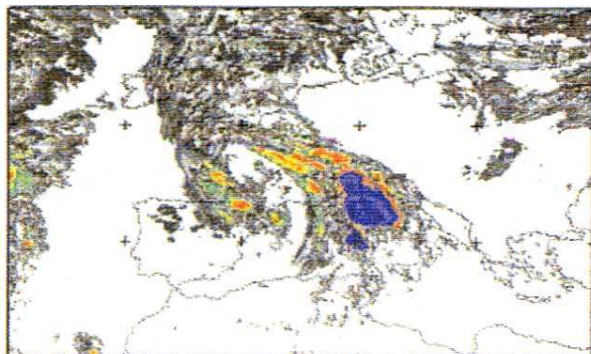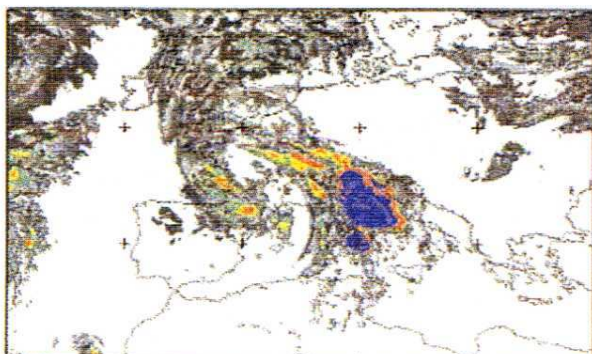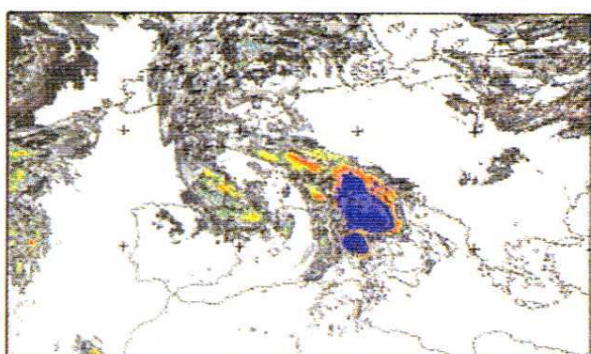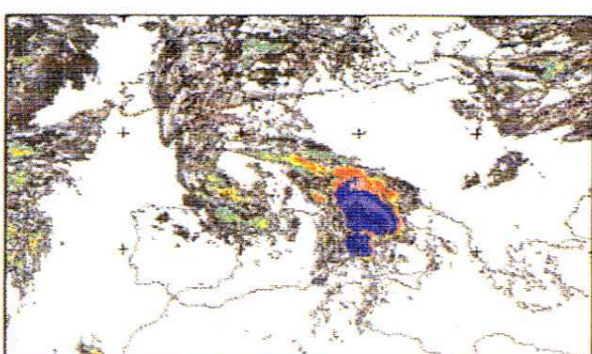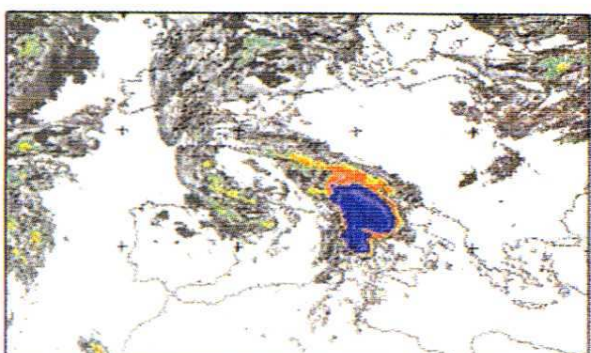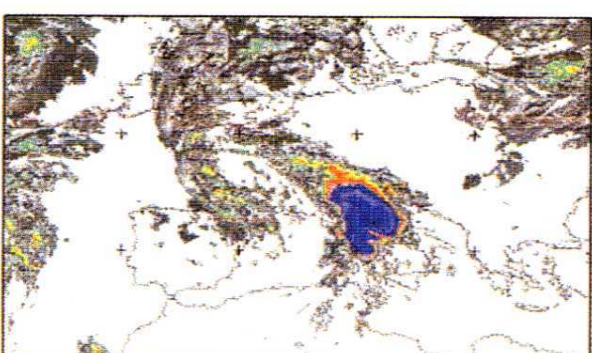
COLOUR PLATE XXVI

FIGURE 9a Sequence of half-hourly Meteosat images in the IR band from 1900 GMT to 2300 GMT of 27 September 1992. (See page 176).
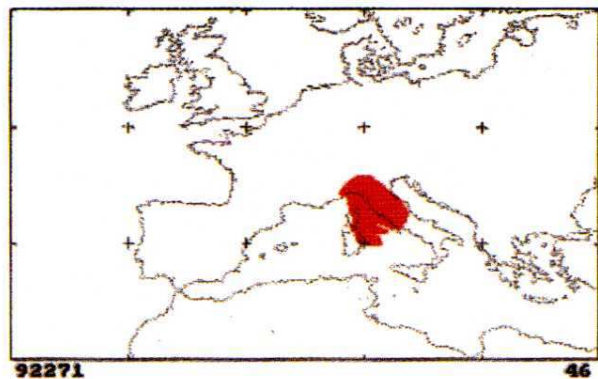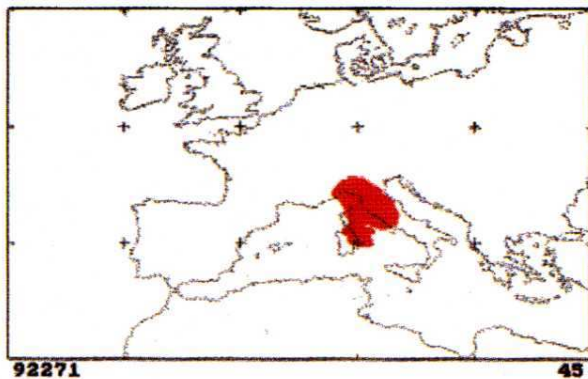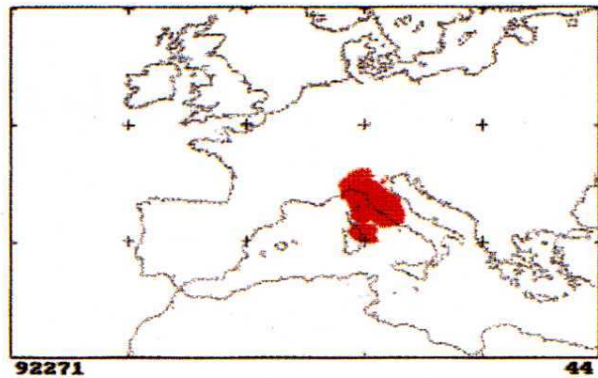
COLOUR PLATE XXVII

FIGURE 9b Cluster identification for the sequence of half-hourly Meteosat images in the IR band from 1900 GMT to 2300 GMT of 27 September 1992. (See page 177).